

# Detectability of Exoplanetary Transits from Radial Velocity Surveys

Stephen R. Kane

*Department of Astronomy, University of Florida, 211 Bryant Space Science Center, Gainesville, FL 32611-2055, USA*

1 February 2008

## ABSTRACT

Of the known transiting extra-solar planets, a few have been detected through photometric follow-up observations of radial velocity planets. Perhaps the best known of these is the transiting exoplanet HD 209458b. For hot Jupiters (periods less than  $\sim 5$  days), the a priori information that 10% of these planets will transit their parent star due to the geometric transit probability leads to an estimate of the expected transit yields from radial velocity surveys. The radial velocity information can be used to construct an effective photometric follow-up strategy which will provide optimal detection of possible transits. Since the planet-harboring stars are already known in this case, one is only limited by the photometric precision achievable by the chosen telescope/instrument. The radial velocity modelling code presented here automatically produces a transit ephemeris for each planet dataset fitted by the program. Since the transit duration is brief compared with the fitted period, we calculate the maximum window for obtaining photometric transit observations after the radial velocity data have been obtained, generalising for eccentric orbits. We discuss a typically employed survey strategy which may contribute to a possible radial velocity bias against detection of the very hot Jupiters which have dominated the transit discoveries. Finally, we describe how these methods can be applied to current and future radial velocity surveys.

**Key words:** stars: planetary systems – methods: observational

## 1 INTRODUCTION

The detection of extra-solar planets in recent years has led to significant advances and challenges in theories regarding planet formation. In particular, planetary migration (Ford & Rasio 2006) and atmosphere models (Burrows, Sudarsky, & Hubeny 2006) have been faced with intense revision in light of the gradually revealed distribution of exoplanetary orbital parameters. The major contribution to revealing this distribution has resulted from large-scale radial velocity surveys, such as those being conducted by the California & Carnegie Planet Search (Marcy et al. 1997) and the High Accuracy Radial velocity Planet Searcher (HARPS) (Pepe et al. 2004) teams. Moreover, the transit method is experiencing increased success through surveys such as the Transatlantic Exoplanet Survey (TrES) (O’Donovan et al. 2006), the XO project (McCullough et al. 2006), the Hungarian Automated Telescope Network (HATNet) (Bakos et al. 2007a), and Super-WASP (Collier Cameron et al. 2007). The improving detection rate from transit surveys is due in no small part to the increasing understanding of optimal photometric meth-

ods for wide-field detectors (Hartman et al. 2004) and the reduction of correlated (red) noise (Pont, Zucker, & Queloz 2006; Tamuz, Mazeh, & Zucker 2005).

Radial velocity measurements of an extra-solar planet provide such information as a lower-limit on the planetary mass along with the orbital period and eccentricity. However, if we are fortunate enough to view the orbit nearly edge-on, then measurements of the planetary transit provide a wealth of complimentary information which reveals the true mass, the radius, and hence the mean density of the planet (Seager & Mallén-Ornelas 2003). The discovery of these transits has thus far been mostly due to the “brute force” approach of wide-field searches, such as those mentioned above. In at least four instances though, the planetary transits were detected for extra-solar planets which were already known via their radial velocity discoveries. These four planets are HD 209458b (Charbonneau et al. 2000; Henry et al. 2000), HD 149026b (Sato et al. 2005), HD 189733b (Bouchy et al. 2005), and GJ 436b (Gillon et al. 2007); the physical characteristics of which span the large diversity seen amongst the short-period ( $< 5$ –10 days) planets known as hot Jupiters. Further attempts have been

made to detect possible transits of certain radial velocity planets (López-Morales et al. 2006; Shankland et al. 2006) which, though unsuccessful, have placed useful constraints on orbital parameters. For those with the interest and the resources to participate in follow-up observations, transit ephemerides for the known radial velocity planets are provided by a useful online resource<sup>1</sup>.

Various current and future radial velocity surveys are predicted to uncover a large number of exoplanets (Kane, Schneider, & Ge 2007). Optimal period analysis and modelling of the data can be used to produce a predicted transit ephemeris. Since the percentage of transiting planets amongst hot Jupiters is around 10% based upon the geometric transit probability (assuming a random distribution of line-of-sight orbital inclinations), it is expected that photometric follow-up of the radial velocity planets will lead to a significant amount of transiting planet discoveries. The error bars on the predicted observing windows will of course increase with the time elapsed since the last data were obtained. It is therefore important to develop an efficient observing strategy for photometric follow-up at the predicted times.

There is an observed difference between the period distributions of planets discovered by the transit method and the radial velocity method (Gaudi, Seager, & Mallen-Ornelas 2005; Butler et al. 2006). Even though the transit method is extremely sensitive to short period planets, the fact that the radial velocity method is also increasingly sensitive to shorter period planets has led to speculation as to how much of the observed difference is real and how much may be attributed to radial velocity selection effects. It is possible that the observing strategy of many radial velocity surveys may contribute to a bias against detecting the very hot Jupiters found by the transit surveys.

This paper presents a summary of how the radial velocity information acquired on an extra-solar planet may be used to construct a photometric follow-up strategy which is optimised towards detecting planetary transits. Section 2 outlines the orbital parameters measurable from radial velocity data and how that leads to a predicted epoch of a planetary transit. Section 3 explains the photometric follow-up strategy, including the transit ephemeris, observing window, and the best telescope/instrument to use for the observations. Section 4 describes a possible correlation of radial velocity observing strategy with the dearth in very hot Jupiter discoveries from radial velocity surveys. Section 5 compares the optimal strategy with other proposed methods and discusses the application of the techniques to various current and future radial velocity surveys for extra-solar planets.

## 2 TRANSIT PREDICTIONS

The radial velocity and transit methods provide complementary information regarding both the orbital parameters of the planet and the physical characteristics of the planet itself. This section describes how, provided the orbital parameters are determined with sufficient accuracy from fitting the

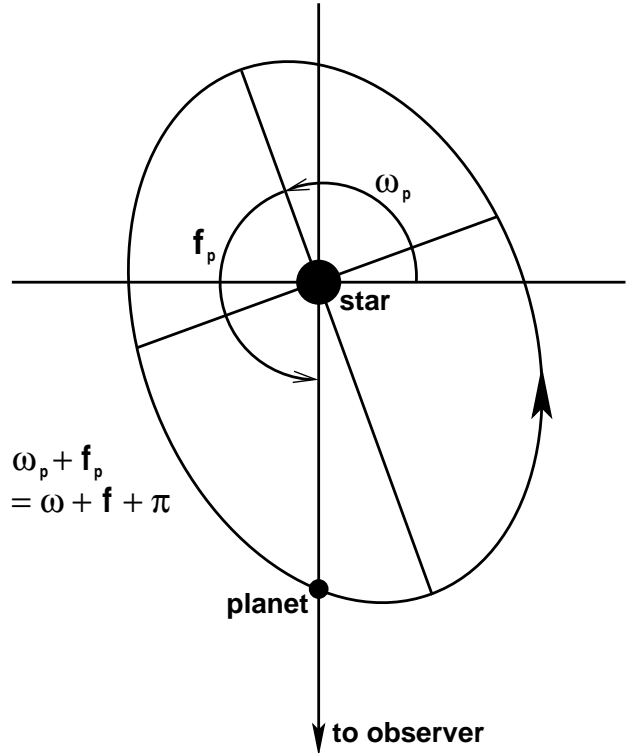


**Figure 1.** A planetary orbit as seen from above, showing the argument of periastron,  $\omega_p$ , and the true anomaly,  $f_p$ .

radial velocity data, the times of possible transit can be predicted.

### 2.1 Complimentary Information

The information provided by radial velocity measurements allows one to construct a model of the planetary orbit which only excludes the orbital inclination. The measured radial velocity of the parent star,  $V$ , is given by

$$V = V_0 + K(\cos(\omega + f) + e \cos \omega) \quad (1)$$

where  $V_0$  is the systemic velocity,  $K$  is semi-amplitude,  $\omega$  is the argument of periastron,  $f$  is the true anomaly, and  $e$  is the eccentricity. The argument of periastron is the angle between the plane of the sky and the position at periastron. The true anomaly is the angle between the position at periastron and the current position in the orbit measured at the focus of the ellipse. The definitions of  $\omega$  and  $f$  for the planet (designated  $\omega_p$  and  $f_p$ ) are demonstrated in Figure 1, where there is a  $\pi$  phase shift relative to  $\omega + f$ . The semi-amplitude of the radial velocity,  $K$ , may be expressed as

$$K = \left( \frac{2\pi G}{P} \right)^{1/3} \frac{M_p \sin i}{M_t^{2/3}} \frac{1}{\sqrt{1 - e^2}} \quad (2)$$

where  $P$  is the period,  $i$  is the inclination of the planetary orbit, and  $M_t = M_p + M_\star$  is the total combined mass of the planet and parent star respectively. The orbital period is also related to the semi-major axis of the planetary orbit,  $a$ , via Kepler's third law:

$$P^2 = \frac{4\pi^2 a^3}{GM_t} \quad (3)$$

<sup>1</sup> <http://www.transitsearch.org/>

Careful fitting of the data and spectral typing of the parent star will therefore lead to estimations of  $M_p \sin i$  along with  $P$  and  $e$ .

Precision photometry obtained during a planetary transit uncovers further information. In particular, the radius of the planet is extracted via the flux difference inside and outside of transit:

$$\frac{\Delta F}{F_0} = \frac{R_p}{R_\star} \quad (4)$$

where  $R_p$  and  $R_\star$  are the radii of the planet and parent star respectively. The complete light curve for the transit including the effect of quadratic limb-darkening can be computed using the formalism shown in Mandel & Agol (2002). The inclination of the orbit is readily resolved since the transit duration,  $t_d$ , depends upon its magnitude:

$$t_d = \frac{P}{\pi} \arcsin \left( \frac{\sqrt{(R_p + R_\star)^2 - (a \cos i)^2}}{a} \right) \quad (5)$$

thus leading to a resolution of the  $M_p \sin i$  ambiguity. Equation (5) applies to the case of a circular orbit, but can be generalised to also apply to eccentric orbits (Tingley & Sackett 2005):

$$t_d = 2R_t \sqrt{1 - \frac{a_t^2 \cos^2 i}{R_t^2}} \frac{\sqrt{1 - e^2}}{1 + e \cos f} \left( \frac{P}{2\pi G M_t} \right)^{1/3} \quad (6)$$

where  $R_t = R_p + R_\star$  is the total combined radii of the planet and parent star. The dependence of the transit duration on the true anomaly in this case leads to a shorter duration near periastron and a longer duration near apastron.

The complimentary nature of the two detection techniques linked by their common determination of the orbital period has lead to a successful partnership of the two methods. In the context of this paper, the most important aspect of the complimentary nature is the usefulness of the constructed orbital model in the prediction of a possible planetary transit. This will be described in detail in later sections.

## 2.2 Transit Probability

Geometrically, the probability of a planet passing between the observer and the planet's parent star is naturally quite low. The probability of an observable planetary transit occurring depends upon the inclination of the planet's orbital plane  $i$  satisfying  $a \cos i \leq R_p + R_\star$ . The transit probability,  $P_t$ , is then given by

$$P_t = \frac{(R_p + R_\star)}{a(1 - e \cos E)} \approx \frac{R_\star}{a(1 - e \cos E)} \quad (7)$$

where  $E$  is the eccentric anomaly. For a circular orbit, this simplifies to  $P_t \approx R_\star/a$  from which it is clear that, as far as the probability is concerned, the size of the planet is of little consequence and the dependence lies mostly upon the size of the parent star and the orbital radius. However, equations (4) and (7) show that the transit method clearly favours large planets orbiting their parent stars at small orbital radii. Thus, many of the hot Jupiters discovered via radial velocity surveys are expected to also exhibit a photometric transit signature.

Figure 2 shows the dependence of the geometric transit probability on semi-major axis and orbital period for

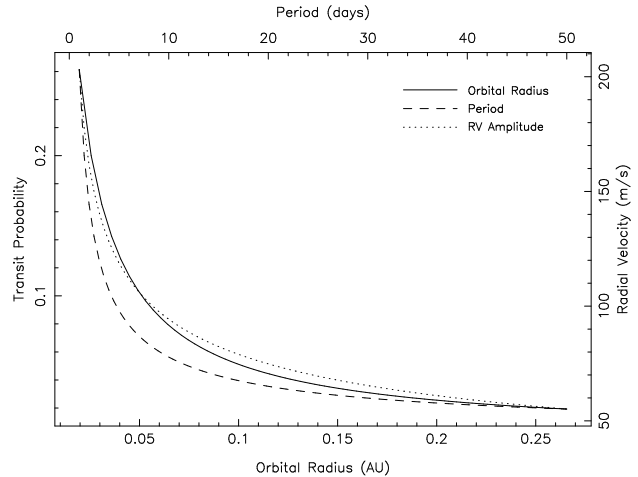


**Figure 2.** The probability of a Jupiter-radius planet transiting a solar-radius star for periods ranging between 1 day and 50 days. The peak radial velocity amplitude exhibited by such a star as a function of period is also plotted as a dotted line.

a Jupiter-radius planet in a circular orbit around a solar-radius star. The transit probability decreases very rapidly with increasing period and leading to an almost negligible probability beyond a 50 day period orbit. Thus, most of the currently known transiting extra-solar planets have periods less than 5 days since this region of period space has by far the highest probability of producing an observable transit. Figure 2 also shows the equivalent peak radial velocity amplitude that would be produced by a transiting Jupiter-mass planet orbiting a solar-mass star as a function of period, assuming a circular orbit. This relation shows a similar dependence on period for the given period range.

According to Lineweaver & Grether (2003), 0.5%–1% of Sun-like stars in the solar neighbourhood have been found to harbour a Jupiter-mass companion in a 0.05 AU (3–5 day) orbit. Assuming that the orbital plane of these short-period planets are randomly oriented, the geometric transit probability is approximately 10%. By performing Monte-Carlo simulations such as those conducted by Kane et al. (2007), one can use this probability to predict the number of observable transits in a given survey field. If the planets are first discovered by the radial velocity method, then one is mostly able to avoid the false-alarm contaminants, such as those described by Brown (2003), that plague purely photometric transit surveys.

## 2.3 Epoch of Planetary Transit

Once a suitable fit is found for the radial velocity data, one can calculate the epoch at which the next planetary transit may occur. For a purely circular orbit, one expects that the transit will occur when the radial velocity of the star is zero (peak-to-peak mid-point) and decreasing. An approximation of this sort will suffice in most cases since the effects of tidal circularization are well observed on hot Jupiters to produce close to zero eccentricity orbits. A notable exception to this has been observed with the high eccentricity of the transiting planet HD 147506b (Bakos et al. 2007b). As described for binary systems by Lecar, Wheeler, & McKee (1976) and compared to exoplan-

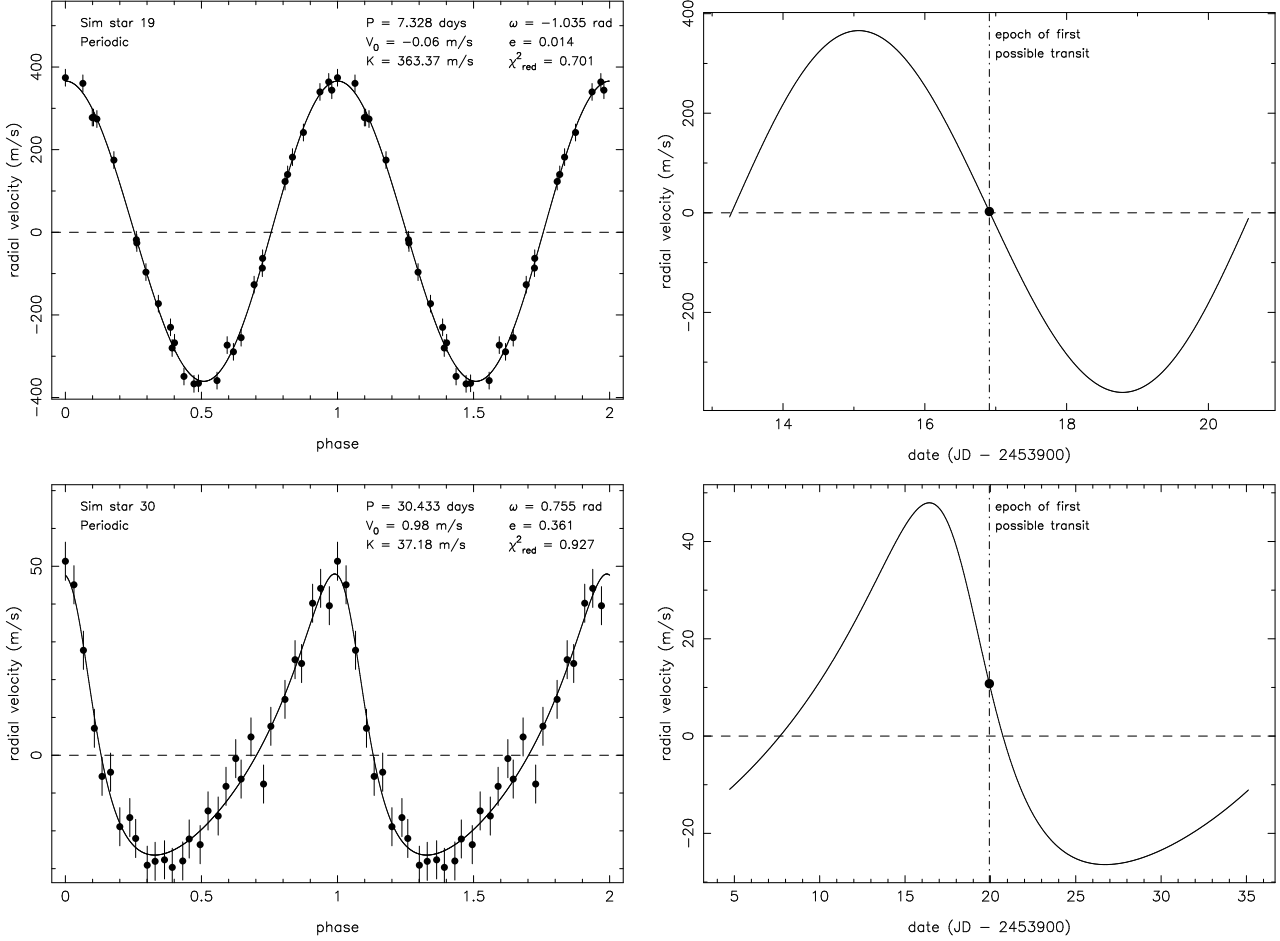


**Figure 3.** The best-fit radial velocity model for two simulated datasets (left), each with an accompanying plot showing the best-fit model with the epoch of a possible transit time (right). The top example is for a short-period circular orbit and the bottom example is for a longer period elliptical orbit.

etary systems by Halbwachs, Mayor, & Udry (2005), the tidal torque varies as  $1/a^6$  leading to a quite severe dependence on period. Beyond the tidal circularization limit of  $\sim 0.1$  AU however, the range of orbital eccentricities becomes extremely broad with little or no dependency on period. A more general description of when a possible transit will occur is defined using the argument of periastron and the true anomaly, as shown in Figure 1. In other words, it is the location in the orbit where  $\omega + f = \pi/2$ . This is true regardless of if the orbit is prograde or retrograde. Minimising the radial velocity function at this location then yields the time of possible transit closest to the times of radial velocity observations.

According to equation (1), the difference in radial velocity between an eccentric and circular orbit at the point of mid-transit is

$$\Delta V = V_e - V_c = K e \cos \omega \quad (8)$$

which can lead to a significant change in the predicted epoch of transit. Moreover, the difference in the time of mid-transit can be calculated by considering the mean anomaly,  $M$ , given by

$$M = \frac{2\pi}{P}(t - t_0) = E - e \sin E \quad (9)$$

where  $t_0$  is the time at periastron. The eccentric anomaly is related to the true anomaly by

$$\cos f = \frac{\cos E - e}{1 - e \cos E} = \cos(\pi/2 - \omega) \quad (10)$$

and allows equation (1) to be evaluated as a function of time. Hence, the difference in time of mid-transit between an eccentric and circular orbit is

$$\Delta t = t_e - t_c = -\frac{P}{2\pi}(e \sin E) \quad (11)$$

where one can evaluate  $E$  by solving equation (9), also known as Kepler's equation.

Figure 3 shows two examples of simulated radial velocity datasets, each with a different planetary signature injected. The top example demonstrates a relatively short-period planet with a typically circular orbit. In this case the predicted epoch of transit occurs exactly when the decreasing radial velocity reaches zero. The bottom example in Figure 3 demonstrates a longer period planet with a substantially eccentric orbit in which the actual transit time falls well outside the observing window of when a circular assumption would have predicted. The magnitude of this time difference depends upon the period, but the predicted

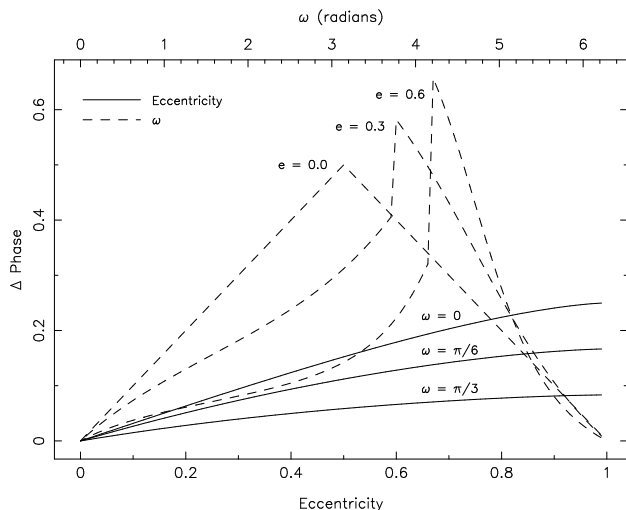


**Figure 4.** The effect of  $\omega$  and  $e$  on the predicted transit time, represented here as a fraction of the phase of the orbit. The solid lines show the effect of  $e$  for three different values of  $\omega$  and the dashed lines show the effect of  $\omega$  for three different values of  $e$ .

time of transit can be in error by more than a day for even a relatively short period. Since longer period planets have a much smaller probability of producing an observable transit, these situations will be relatively uncommon. However, considering searches in this region of parameter space have already been conducted and future surveys will undoubtedly be further exploring this region, the eccentricity of the orbit must be taken into account.

### 3 PHOTOMETRIC FOLLOW-UP STRATEGY

This section describes how the radial velocity data and the predicted transit times can be used to construct a complete follow-up observing strategy which is optimised for the particular target star.

#### 3.1 Transit Ephemeris

Kane et al. (2007) describes in detail a radial velocity simulation code called *rvsim*. One of the primary functions of this code is to ingest large amounts of precision radial velocity data which can then be automatically sifted for planetary signatures. The code also produces fits to the planetary signals and provides transit ephemerides based on the methods presented in the previous section. This is performed by first calculating the radial velocity which satisfies  $\omega + f = \pi/2$ . A grid search is then used to locate the approximate time at which this occurs after the first radial velocity measurement was obtained. Since this is a computationally inexpensive algorithm, the grid precision can be exceptionally high without loss of performance leading to an accurate estimate of predicted transit epoch based on the fit parameters.

It has been already mentioned that the eccentricity of the orbit can have a significant effect on the time of transit. It is also clear from the definition of when an observable transit is predicted to occur and also from Figure 1 that the ephemeris calculation is heavily dependent upon the estimate of  $\omega$ . These two parameters tend to have a high degree

of uncertainty when relatively few data points are available to produce a fit. The amplitude of the effect of the predicted transit time is demonstrated in Figure 4 in which the change in transit time (represented as a fractional amount of the phase or period) is plotted as a function of eccentricity and  $\omega$ . Clearly these effects can become significant for even relatively small uncertainties. For example, of the 172 planets tabulated in Butler et al. (2006), 124 have  $\omega$  uncertainties shown. The mean value of these uncertainties is  $20^\circ$  and the median is  $10^\circ$ . For a circular orbit and a period of 4 days, a shift of  $10^\circ$  in the value of  $\omega$  will lead to a 3 hour difference in the predicted time of mid-transit. Similarly, for a 4 day orbit with  $e = 0.3$ , a shift of  $10^\circ$  in the value of  $\omega$  leads to a 2.5 hour difference. Constraining the values of  $e$  and  $\omega$  is therefore of critical importance before constructing a reliable transit ephemeris.

As pointed out by Wittenmyer et al. (2005), even very precise measurements of the orbital period contain errors which propagate into larger uncertainties in the ephemeris. This can take place in a relatively short period of time; a period error of  $\sim 1$  second will lead to an ephemeris uncertainty of several minutes for hot and very hot Jupiters after only one year. Thus, though the uncertainty in  $e$  and  $\omega$  can cause problems in predicting the epoch of first transit, the error associated with the period has a cumulative effect on the transit ephemeris. In the case of HD 189733b, we are fortunate that detectable transits exist in the Hipparcos data which have allowed the period to be determined with an accuracy of less than 1 second (Hébrard & Lecavelier des Étangs 2006). Maintaining an accurate ephemeris is important not only for future observations, but for the possible detection of additional planets through transit timing observations (Agol et al. 2005). Fortunately, “re-alignment” of the transit ephemeris can always be re-established through further radial velocity observations to re-predict the next transit event and further refine the period.

#### 3.2 Transit Duration and Observing Window

The predicted point of mid-transit at a particular epoch is only as accurate as the robustness of the fit to the radial velocity data, in particular the period, and the elapsed time since the most recent radial velocity measurements were obtained. The size of the observing window to ensure complete coverage of the transit can be estimated based on this information. Assuming that the values of  $e$  and  $\omega$  are well constrained, as described in the previous section, the observing window is defined by (a) the transit duration, (b) the uncertainty in the measured period, and (c) the number of periods elapsed since the predicted epoch of first transit. The dominant factor out of these is normally the transit duration, which is given by equation (6). Figure 5 shows the variation in observing window with period, including the effects of period uncertainty ( $3\sigma$  either side of the transit duration) for an elapsed time of 20 orbits and 50 orbits. This example assumes a Jupiter-radius planet in a circular orbit transiting a solar-radius star with a period uncertainty of  $\sim 5$  seconds. The effect of eccentricity can be to increase or decrease the transit duration by as much as 50% up to an eccentricity of  $\sim 0.5$ , depending on the true anomaly at the time of transit. This necessitates a proportional change in the size of the observing window.

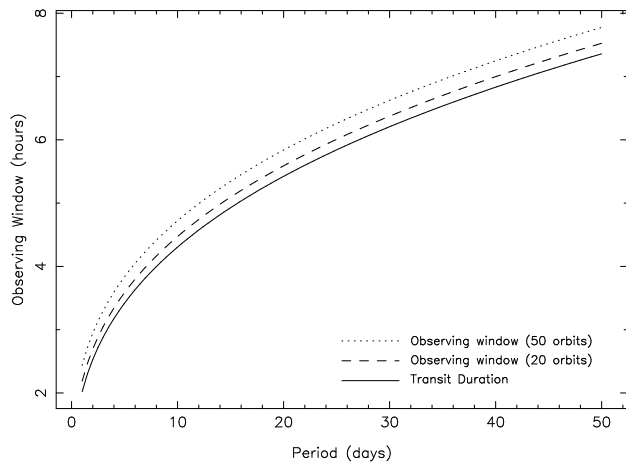


**Figure 5.** The observing window for detecting the transit of a Jupiter-radius planet orbiting a solar-radius star for periods ranging between 1 day and 50 days. The solid line shows the transit duration. The dashed and dotted lines include the additional effect of the period uncertainty for 20 and 50 orbits respectively after the last measurements were acquired.

Even though the period of the planetary orbit can be quite accurately determined, the transit duration will have a much larger associated uncertainty. It was shown by Kane et al. (2005) that the duration of an exoplanetary transit is relatively insensitive to the spectral type of the parent star as compared to the effect of increasing orbital radius, and so the observing window shown in Figure 5 is fairly representative. However, it is clear from equation (6) that the estimated transit duration for a given orbital radius can depend heavily upon the stellar radius estimate deduced from the spectral type. An example of this can be seen in the detections of WASP-1b and WASP-2b (Collier Cameron et al. 2007) where the difficulty presented by spectral typing imposed large uncertainties on the stellar radius estimates. As such, the observing window should be calculated based upon the assumption that the maximum estimates stellar radius and hence the maximum estimated transit duration applies.

### 3.3 Rossiter-McLaughlin effect

The Rossiter-McLaughlin (RM) effect (McLaughlin 1924; Rossiter 1924) is a well-known phenomenon observed for many eclipsing binary star systems, and has also been predicted and observed in the radial velocity data acquired during exoplanetary transits (Ohta, Taruya, & Suto 2005). Furthermore, the confirmation of transiting planets and measurement of planetary orbital alignments using the RM effect has been discussed in detail by Gaudi & Winn (2007). Since a planetary transit is able to manifest its presence in the radial velocity data, the RM effect allows the remarkable opportunity to discover transiting planets through spectroscopic means, as was the case for HD 189733 (Bouchy et al. 2005).

With respect to the impact the RM effect will have on the predicted transit ephemeris, this depends upon the model used for the radial velocity data and the percentage of data points which are obtained inside of the transit. As described in Ohta et al. (2005), it is relatively trivial to

include the RM effect in the model being used to fit the radial velocity data. On the other hand, for hot Jupiters the transit duration is typically 3–4 hours which is 3–5% of the total orbital period. Since there will be a correspondingly small number of RM effect measurements in the complete dataset, it is possible to exclude these measurements from the fit without compromising the orbital parameters extracted from the model fit. This is the approach which was taken by Sato et al. (2005) who also noted the small probability that they should acquire radial velocity data during the transit of the hot Saturn orbiting HD 149026.

To determine the effect the RM effect has on the transit ephemeris, we produced an independent fit to the radial velocity data published by Sato et al. (2005). These data contain 4 measurements during a transit, a remarkably large fraction of the 11 total data points. Including these measurements in the fit yields a period of  $P = 2.8767 \pm 0.002$  days and a semi-amplitude of  $K = 43.1 \pm 1.7$  m s<sup>-1</sup>. Computing the transit ephemeris from this fit produced predicted mid-transit times of  $t_1 = 2453504.869$ ,  $t_2 = 2453527.883$ , and  $t_3 = 2453530.759$ . When compared to the actual times of mid-transit measured by Sato et al. (2005), the differences are  $\Delta t_1 = 0.004$  days,  $\Delta t_2 = 0.019$  days, and  $\Delta t_3 = 0.008$  days. This is equivalent to differences of between 5 and 30 minutes. These differences can be completely accounted for by the respective fit parameters obtained and the cumulative stacking of the period uncertainty. Therefore in this case the RM has had little effect on the transit ephemeris although a larger amplitude RM effect with a comparable number of data points could prove fatal for transit predictions attempted significantly after the radial velocity data is obtained. In such cases an iterative elimination of radial velocity measurements within the transit window (sigma-clipping) can enable a more accurate prediction of the transit ephemeris.

### 3.4 Transit Detectability

The overwhelming majority of known radial velocity planets have been detected as companions to stars with a magnitude of  $V < 14$ . Given the large number of wide-field transiting planet surveys being conducted, it is possible that a newly detected radial velocity planet will have already been monitored by one or more of the surveys. However, large areas of the sky remain to be monitored with significant time resolution and the phase coverage of transits that are present in the data are likely to require follow-up observations. Therefore, the optimal approach is to design a custom observing program which takes into account the magnitude of the star and the required signal-to-noise (S/N) for an unambiguous detection.

To demonstrate this, we design a simple example using a generic telescope and detector. The telescope in this example is assumed to have a 1.0m aperture, representative of the many under-subscribed 1.0m class telescopes which are generally excellent choices for these observations. A typical detector would have characteristics similar to a Tek 2K CCD, which for this example is assigned a gain and readout noise of 2.4 e<sup>-</sup>/ADU and 3.9 ADU respectively. It is also assumed that a standard Cousins *R* filter with a bandwidth of  $\sim 1500$  Å is used with a total quantum efficiency of 50%.

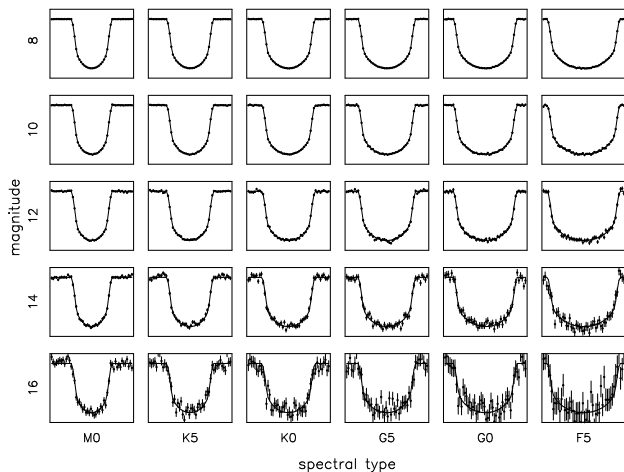


**Figure 6.** Model transit lightcurves overlaid with simulated data from a generic 1.0m telescope and detector for a range of spectral types and magnitudes. This assumes a Jupiter-radius planet transiting a solar-radius star.

The noise model used takes into account detector characteristics as well as photon statistics and takes the form

$$\sigma^2 = \sigma_0^2 + \frac{(f_\star + f_{\text{sky}})\Delta t}{g} \quad (12)$$

where  $\sigma_0$  and  $g$  are the CCD readout noise (ADU) and gain ( $e^-/\text{ADU}$ ) respectively,  $f_\star$  and  $f_{\text{sky}}$  are the star and sky fluxes respectively, and  $\Delta t$  is the exposure time. For this simulation, we adopt an exposure time of 30 seconds under grey time conditions.

The photometric accuracy will be limited by the number of suitable comparison stars available within the instrument field-of-view (FOV). For a detector such as the one used in this example, the typical pixel scale is 0.4 arcsec/pixel giving a total FOV of  $\sim 186$  square arcmins. Using the star counts for the Kepler field presented by Kane et al. (2007), the number of stars per square degree is  $\sim 96$  for  $V < 12$  and  $\sim 247$  for  $V < 13$ . This leads to an estimate of  $\sim 5$  stars in the FOV for  $V < 12$  and  $\sim 12$  stars in the FOV for  $V < 13$ . Even for relatively bright targets, the integration times can be adjusted to allow for sufficient differential photometry comparison stars for in most cases. If this is not possible, then carefully considering an instrument with a larger FOV may be required.

Shown in Figure 6 are model transits and simulated data for a range of magnitudes and spectral types assuming a single transit by a Jupiter-radius planet. The plot windows have been normalised to a width of  $3R_\odot/R_\star$ , equivalent to the projected path of the planet as it crosses the stellar disk, and a normalised depth for ease of comparison of photometric accuracy. Transits of late-type stars, particularly M stars, are of shorter duration but are considerably deeper and so produce a much higher S/N during the transit. However, radial velocity surveys typically concentrate on F–G–K stars for their brightness, frequency, and stability properties. This simulation shows that conducting a suitable follow-up observing program with reasonably accessible 1.0m class telescopes can lead to rapid confirmation or elimination of observable planetary transits down to a magnitude depth which is beyond most radial velocity surveys.

The issues of red noise (Pont et al. 2006) and stellar micro-variability (Aigrain, Favata, & Gilmore 2004) have presented serious challenges to transit surveys. Various tools have been developed to overcome these obstacles, such as the SysRem algorithm developed by Tamuz et al. (2005) which is now commonly used to minimise systematic effects in the photometry. The major way in which these problems affect transit surveys is by generating false alarms of a quantity which is at least an order of magnitude greater than the expected number of real transit signatures. This becomes a problem that must be solved by an efficient transit detection algorithm and a reliable set of rejection criteria. These photometric calibration effects will also be present in the follow-up photometric data of known radial velocity planets. These data have two key advantages however. Firstly, many of the systematic noise properties of transit surveys are due to the wide-fields, such as the position-dependent airmass, colour, and point-spread function (PSF). These are present to a much lesser extent in instrument designs such as the one presented here. Also, since one only needs to observe during the predicted observing window, these observations suffer far less from night-to-night variations which contribute greatly to the red noise of transit surveys. Secondly, searching for transits in the photometry of a single star is a very different problem than deriving an automated method for scanning many thousands of stars. The targeted nature of single-star follow-up allows for a much more thorough search of the photometry to be conducted.

#### 4 THE RADIAL VELOCITY BIAS

The currently known period distribution of extra-solar planets exhibits a pileup of planetary periods which occurs near 3 days. This has been clearly demonstrated by, for example, Butler et al. (2006). The mechanism of planetary migration (Rice & Armitage 2005) plays a major role in explaining much of the period distribution observed for hot Jupiters. However, it has also been observed that, although the radial velocity method is more sensitive to planets at small orbital radii, the transit method has managed to uncover very hot Jupiters (less than 3 day periods) which remained hidden to the radial velocity surveys. It has been a matter for debate whether this lack of radial velocity very hot Jupiters is an observational bias or selection effect or if it is indeed a reflection of the real period distribution (Gaudi et al. 2005). In other words, the transit detection of very hot Jupiters may simply be due to the relatively high probability of detecting planets at very small orbital radii even though such planets are quite rare. In this section I discuss some of the radial velocity biases against detection of planetary periods close to 1 day.

There are a variety of factors which can possibly contribute to an overall bias of radial velocity surveys against detecting 1 day or even 2 day period planets. Transit surveys are of course very strongly biased towards detecting shorter period planets due to the geometric transit probability being so much higher in this regime. In fact there is also a slight bias towards detecting planets via the transit method around small (late-type) stars since the depth of the transit lightcurve is significantly larger. This bias has thus far been balanced by the difficulties imposed in achieving sufficient

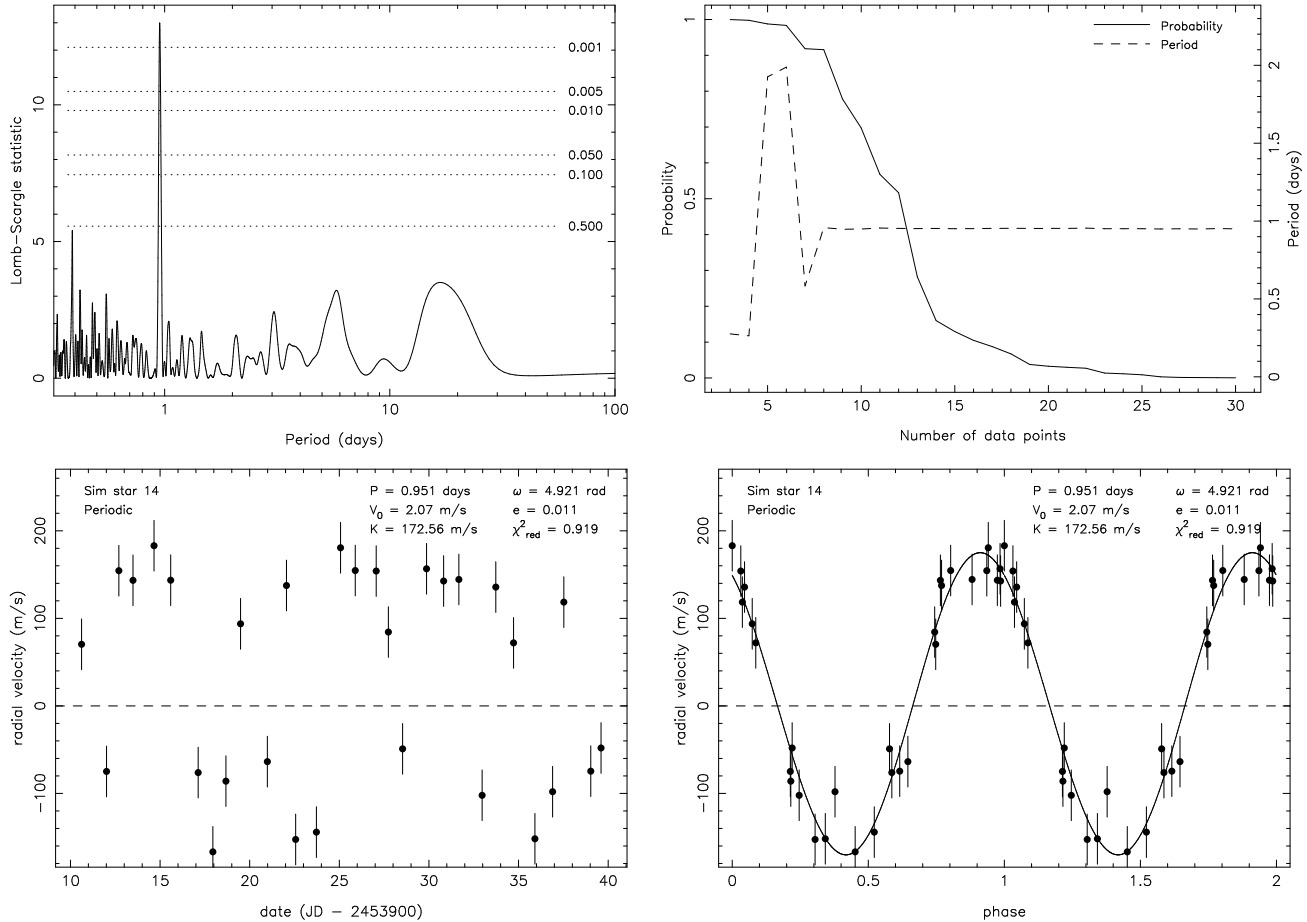


**Figure 7.** An example of a  $\sim 1$  day period planet observed for 30 consecutive nights. The time of observation each night is randomized by passing identical times through a 4 hour gaussian filter. The resulting periodic signal in this case is easily recovered, as shown by the periodogram (top-left). The probability of the strongest period being a false-alarm drops significantly beyond  $\sim 8$  data points (top-right). The unfolded (bottom-left) and folded data with best-fit model (bottom-right) are also shown.

photometric precision of M dwarfs and also that magnitude-limited wide-field transit surveys tend to be dominated by a similar distribution of F–G–K stars as those surveyed by radial velocity experiments. The smaller Roche limit for M dwarfs may also be useful in explaining the difference in period distributions of the transit and radial velocity surveys though, as pointed out by Ford & Rasio (2006), the current small number statistics of the known transiting planets limits such an investigation.

One of the main contributing factors to the radial velocity bias is undoubtedly the adopted observing strategy of the survey in question. A typical survey strategy will obtain one data point per target per night. In addition, it is also typical to use the same observing schedule each night, usually to secure observations when the target is closest to the zenith and hence at minimum airmass. In the case where several observations are obtained for a single target on a single night, these are often binned together to produce a single high S/N image. This results in effectively observing the target at approximately the same time every night.

In principle, observing a target once per day does not immediately exclude 1 day period planets from detection. Figure 7 shows an example of a case in which a planetary

signature with an approximately 1 day period is easily recovered relatively quickly during 30 consecutive nights of observations. The times of observation for the simulated data were produced by taking an identical time of observation for each night and then passing each time through a gaussian filter with a standard deviation of 4 hours. This method of randomizing the time of observation results in a large variation of observing times from night to night. The top-right plot in Figure 7 shows the dramatic drop in false-alarm probability on a significant period estimate beyond  $\sim 8$  data points, at which point the estimate has settled upon the correct 1 day period.

The particular aspect of the observing strategy with the most impact is the change in observing time per target per night. A quantitative estimate of this impact was calculated by performing a Monte-Carlo simulation which produced several thousand simulated radial velocity datasets containing planetary signatures with periods between 0.9 and 1.1 days. The datasets assumed 30 consecutive nights and the time of observation each night was passed through a gaussian filter with a standard deviation ranging from 1 to 4 hours. A weighted Lomb-Scargle periodogram was calculated for each dataset and the difference in false-alarm



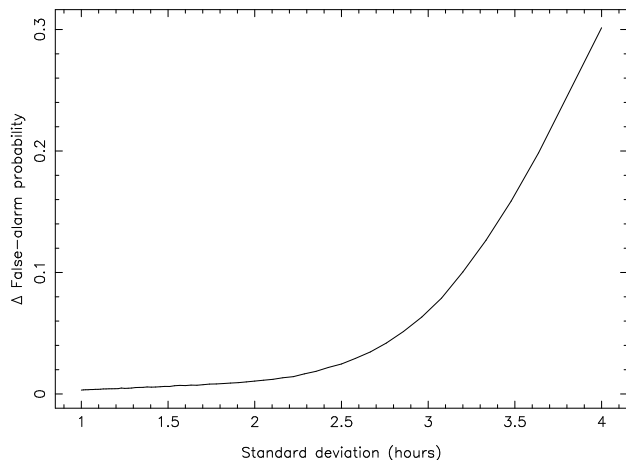


**Figure 8.** The change in the difference between the two highest periodogram peaks as a function of the standard deviation in the time of observation. The quality of the period determination steadily increases when the target is observed at significantly different times each night.

probability between the two highest peaks was used as a quality estimate into the ambiguity of the period. Through this simulation, an assessment of the effect of observing time on the likelihood of planet detection was produced.

Figure 8 shows the results of the simulation. As demonstrated by Figures 7 and 8, the chances of being able to reliably determine the period of a short period planet are exceptionally high when times of observations are sufficiently scattered between nights. However, when the times of observations are quite close, within an hour of each other for example, then the periodogram begins to be plagued with aliases. Thus, increasing the time range over which data is obtained for a particular target greatly reduces the relative strength of contaminating period aliases. It is often the case that 1 day period aliases are discarded from radial velocity surveys due to their ambiguous nature. The signature of planets with periods close to 1 day are then particularly vulnerable to the effect shown in Figure 8. Transit surveys also suffer contamination by 1 day period aliases, though this is due to factors such as night-to-night variations and red-noise rather than the sampling intervals.

There is a chance also of missing two day period planets if observations only occur (either due to weather or other interruptions) every other day. The effect is compounded by the fact that most radial velocity surveys only observe a target long enough to ascertain if the target is variable. This is typically assessed after a handful (5–10) of data points have been acquired. The effect described here certainly does not completely account for the lack of very hot Jupiters detected via radial velocity surveys. By providing a quantitative estimate of the effect however, modifying observing strategies accordingly may improve sensitivity to those planets in the future. Solutions to the problem depend upon the times at which the target is observable and will usually compromise observing time. An example is to observe the target at a similar airmass either side of the meridian.

## 5 DISCUSSION

The rate at which radial velocity planets are being discovered is increasing, a trend which is expected to continue as next-generation radial velocity surveys are realised. Considering the high number of expected hot Jupiters from current and future surveys, the techniques presented here will be useful in planning follow-up photometric observations of targets. Provided these follow-up observations of the planet candidates are conducted within a reasonably short time interval, the predicted transit windows will allow swift confirmation of whether or not the planet’s orbit is favourably inclined for transits to be visible.

Surveys such as that being conducted by the N2K Consortium (Fischer et al. 2005) are already employing such techniques, and has allowed them to make at least one successful transit detection (Sato et al. 2005). The methods presented here are part of an end-to-end system which allows the entire follow-up observing program to be designed around the information available from the radial velocity measurements and produced in a semi-automated fashion. The *rvsim* code mentioned here and described further in Kane et al. (2007) was used, for example, in calculating the predicted transit ephemeris for HD 102195b (Ge et al. 2006a). Follow-up observations were conducted during the predicted transit windows using an Automatic Photoelectric Telescope (Henry 1999) located at Fairborn Observatory. These observations rule out transits of the planetary companion.

The probability of an exoplanet transiting its parent star increases dramatically with decreasing period. Perhaps ironically, the very hot Jupiters with the highest geometric transit probability remain elusive to the radial velocity surveys. This may be helped slightly by designing an observing schedule which uses a large scatter in observing times on consecutive nights, although this only applies to planets whose period are close to a small integer number of days. Once radial velocity surveys begin to uncover these ultra-short period planets, the number of transiting planets detected via the radial velocity method will correspondingly increase. Even so, radial velocity planets with periods close to an integer number of days are difficult to follow-up photometrically because the transit phasing shifts very slowly with respect to the night-day occurrence.

There are several multi-object radial velocity surveys for extra-solar planets which are currently underway, using such facilities as GIRAFFE and FLAMES-UVES on the VLT (Loeillet et al. 2007) and a dispersed fixed-delay interferometer instrument, called the Keck ET (Ge et al. 2006b), on the Sloan Digital Sky Survey 2.5m telescope (Gunn et al. 2006). The use of these instruments to survey such fields as the Kepler field, as suggested by Kane et al. (2007), will provide invaluable information for the Kepler mission (Basri, Borucki, & Koch 2005) regarding stars with companions; whether they be planetary or stellar in nature. In particular, photometry of suspected long-period planets for which only a handful of transits are observed will benefit greatly from existing radial velocity data which are able to immediately confirm their planetary nature. Considering that Kepler is expected to discover planets with periods larger than 1 year during the mission lifetime, this is an important factor to consider.

## 6 CONCLUSIONS

Simple calculations based upon the frequency of hot Jupiters and the geometric transit probability show that around 0.1% of solar-type stars should have a detectable transit due to an extra-solar planet. In practise however, the number of transiting planets detected via transit surveys is much reduced, largely due to the issues of false positives and correlated “red” noise. This paper describes strategies for efficient photometric follow-up of radial velocity planets to maximise the number of transit discoveries. Since the target star is known to harbour a planet, the transit detection is unaffected by many of the problems posed by blind transit surveys and is simply limited by the transit probability.

The radial velocity and transit techniques of exoplanet detection are complimentary in the information they provide regarding orbital and physical parameters. For longer period planets, there is an increasing chance of orbital eccentricity which can significantly alter the predicted time of transit. Though the transit probability decreases in this regime, the expected increase in planet discoveries at longer orbital periods will lead to transiting planets found in eccentric orbits. The transit window must also be handled with care, in particular taking into account the increase in window size due to the period uncertainty. The fortran code *rvsim* is designed to automatically ingest, test for periodicity, and fit models to large amounts radial velocity data from planet surveys. In addition, a transit ephemeris is computed together with the observing windows, and the required S/N for successful detection is estimated. In this way, an end-to-end process has been constructed which is able to produce a customised observing campaign complete with the telescope and instrument requirements. We present an example using a 1.0m telescope, the class of which is relatively available and make an ideal choice for fast follow-up of stars with known radial velocity planets.

The discovery of transiting planets can be increased with improved observing strategies for radial velocity surveys which eliminate any biases against 1–2 day period planets. We have demonstrated a possible cause for such a bias and have suggested a programmed observing schedule which increases the standard deviation in the times of observation. The ultimate goal is to facilitate a radial velocity survey design in such a way that they are more efficient at detecting very hot Jupiters which of course have the highest chance to transit their parent star.

Although the detection of transiting planets via radial velocity surveys is largely free from the observational biases which plague “blind” transit surveys, the true distribution of transiting planets probably won’t be fully realised until missions such as Kepler begin their much anticipated observations. These surveys are not without their own biases, but the large expected number of transiting planets detected will yield unprecedented insight into the formation and properties of these short-period planets.

## ACKNOWLEDGEMENTS

The author would like to thank Suvrath Mahadevan, Julian van Eyken, Scott Fleming, and Robert Wilson for several useful discussions. The author is also grateful for the constructive suggestions of the referee.

## REFERENCES

- Agol, E., Steffan, J., Sari, R., Clarkson, W., 2005, MNRAS, 359, 567
- Aigrain, S., Favata, F., Gilmore, G., 2004, A&A, 414, 1139
- Bakos, G.A., et al., 2007a, ApJ, 656, 552
- Bakos, G.A., et al., 2007b, ApJ, submitted (astro-ph/0705.0126)
- Basri, G., Borucki, W.J., Koch, D., 2005, New Astron. Rev., 49, 478
- Bouchy, F., et al., 2005, A&A, 444, L15
- Brown, T.M., 2003, ApJ, 593, L125
- Burrows, A., Sudarsky, D., Hubeny, I., 2006, ApJ, 650, 1140
- Butler, R.P., et al., 2006, ApJ, 646, 505
- Charbonneau, D., Brown, T.M., Latham, D.W., Mayor, M., 2000, ApJ, 529, L45
- Collier Cameron, A., et al., 2007, MNRAS, 375, 951
- Fischer, D.A., et al., 2005, ApJ, 620, 481
- Ford, E.B., Rasio, F.A., 2006, ApJ, 638, L45
- Gaudi, B.S., Seager, S., Mallen-Ornelas, G., 2005, ApJ, 623, 472
- Gaudi, B.S., Winn, J.N., 2007, ApJ, 655, 550
- Ge, J., et al., 2006a, ApJ, 648, 683
- Ge, J., et al., 2006b, Proc. SPIE, 6269, 75
- Gillon, M., et al., 2007, A&A, in press (arXiv:0705.2219)
- Gunn, J.E., et al., 2006, AJ, 131, 2332
- Halbwachs, J.L., Mayor, M., Udry, S., 2005, A&A, 431, 1129
- Hartman, J.D., Bakos, G., Stanek, K.Z., Noyes, R.W., 2004, AJ, 128, 1761
- Hébrard, G., Lecavelier des Étangs, A., 2006, A&A, 445, 341
- Henry, G.W., 1999, PASP, 111, 845
- Henry, G.W., Marcy, G.W., Butler, R.P., Vogt, S.S., 2000, ApJ, 529, L41
- Lecar, M., Wheeler, J.C., McKee, C.F., 1976, ApJ, 205, 556
- Kane, S.R., Collier Cameron, A., Horne, K., James, D., Lister, T.A., Pollacco, D.L., Street, R.A., Tsapras, Y., 2005, MNRAS, 364, 1091
- Kane, S.R., Schneider, D.P., Ge, J., 2007, MNRAS, 377, 1610
- Lineweaver, C.H., Grether, D., 2003, ApJ, 598, 1350
- Loeillet, B., et al., 2007, A&A, submitted (astro-ph/0703725)
- López-Morales, M., Morrell, N.I., Butler, R.P., Seager, S., 2006, PASP, 118, 1506
- Mandel, K., Agol, E., 2002, ApJ, 580, L171
- Marcy, G.W., Butler, R.P., Williams, E., Bildsten, L., Graham, J.R., Ghez, A.M., Jernigan, G., 1997, ApJ, 481, 926
- McCullough, P.R., et al., 2006, ApJ, 648, 1228
- McLaughlin, P.R., 1924, ApJ, 60, 22
- O’Donovan, F.T., et al., 2006, ApJ, 651, L61
- Ohta, Y., Taruya, A., Suto, Y., 2005, ApJ, 622, 1118
- Pepe, F., et al., 2004, A&A, 423, 385
- Pont, F., Zucker, S., Queloz, D., 2006, MNRAS, 373, 231
- Rice, W.K.M., Armitage, P.J., 2005, ApJ, 630, 1107
- Rossiter, R.A., 1924, ApJ, 60, 15
- Sato, B., et al., 2005, ApJ, 633, 465
- Seager, S., Mallén-Ornelas, G., 2003, ApJ, 585, 1038
- Shankland, P.D., et al., 2006, ApJ, 653, 700
- Tamuz, O., Mazeh, T., Zucker, S., 2005, MNRAS, 356, 1466

Tingley, B., Sackett, P.D., 2005, ApJ, 627, 1011  
Wittenmyer, R.A., et al., 2005, ApJ, 632, 1157